Research Journal of Applied Sciences, Engineering and Technology 5(2): 680-688, 2013
DOI:10.19026/rjaset.5.5009
ISSN: 2040-7459; E-ISSN: 2040-7467

Submitted: May 30, 2012 Accepted: June 21, 2012 Published: January 11, 2013

**Research Article**

# Study of Shielding Properties of a Rectangular Enclosure with Apertures Having Different Shapes but Same Area Using Modal Method of Moments

[1,2]Chao Zhou and [1]Ling Tong
[1]School of Automation, University of Electronic Science and Technology of China, Chengdu 610054, China
[2]Aviation Engineering Institute, Civil Aviation Flight University of China, Guanghan Sichuan 618307, China

**Abstract:** In this study, electric field Shielding Effectiveness (SE) of rectangular enclosure with apertures illuminated by vertical polarization plane wave has been studied by using modal method of moment technique. Electric field SE of enclosure with different shape apertures but same area has been calculated at three different points inside enclosure. To achieve this, assuming appropriate electric field distribution on the aperture, fields inside the cavity are determined using rectangular cavity Green's function. Electromagnetic fields outside the cavity and scattered due to the aperture are obtained using the free space Green's function. Matching the tangential magnetic field across the apertures, the integral equation with aperture fields as unknown variables is obtained. A very good agreement among the results of the proposed technique, results available in the literature and experimental results is observed. The simulation results show that the electric field SE is seriously affected by calculation points, aperture shape and the number of aperture. It has been shown that usual assumption made in EMC literature that lower electric field SE near the aperture than at location inside the enclosure farther away from the aperture is not always true to square aperture at some frequency and square aperture has higher electric field SE than rectangular apertureeven though they have same area.

**Keywords:** Green's function, MoM, rectangular enclosure, Single aperture, Shielding Effectiveness (SE)

## INTRODUCTION

Shielding enclosures are utilized to hinder electromagneticleakage from electronic equipment and as well to protectsensitive instruments against external interference and hence meet the Electromagnetic Compatibility (EMC) standard. The ability of a shielding enclosure to do thisis characterized by its shielding effectiveness which is the ratio of the field strength in thepresence and absence of the enclosure for both electric andmagnetic fields. SE is primarily affected by the wavepenetration through apertures and slots used toaccommodate visibility, ventilation or access to interiorcomponents, such as input and output connections,heat dispersion panels, control panels, visual-access windows, etc. Whatis more, those openings allow exterior electromagnetic energy to penetrate tothe inside space, where they may couple onto Printed Circuit Boards (PCBs), then resulting inthe inner field resonance and the shielding performance being degraded.

Several analytical and numerical methods to calculate shielding effectiveness of metallic enclosures with apertures have been suggested in past years. However, each technique has advantages and disadvantages with respect to other techniques. Pure analytical methods are accurate but can be applied only to various simplifying geometries with some approximations whose validity may be questionable at high frequencies.

For electrically small apertures, (Bethe, 1944) derived a small hole theory, which states that the electromagnetic fields at both sides of a zero-thickness wall with an electrically small aperture represented by an electric and a magnetic dipole illuminated by a plane wave. The relationship between the dipole moments of these dipoles to the original fields is described by polarizability that are functions of the size and shape of the small apertures. Bethe's solution is applicable only to simple geometries (McDonald, 1985) and for complex shapes, numerical techniques are needed (Arvas and Harrington, 1983). Mendez generalized Bethe's theory, for EM radiation from rectangular enclosures with an aperture excited by a center-fed thin dipole and a square loop (Mendez, 1974; Mendez, 1978). However, his formulation is limited to

**Corresponding Author:** Chao Zhou, School of Automation, University of Electronic Science and Technology of China, Chengdu 610054, China

frequencies below the lowest enclosure resonance. Small hole approximation and its generalization application are the primary studies on the subject.

Robinson *et al.* (1996) and Robinson *et al*. (1998) introduced a very simple analytical method based on transmission line model. However, this approach is limited by the assumption of thin apertures, simple geometries, negligible mutual coupling between apertures and fields can be calculated only at points in front of the aperture. The transmission line model was later extended to include higher order cavity modes (Belokour *et al*., 2001) and the effects of loading due to electrical circuits within the enclosure (Thomas *et al*., 1999).

In addition, some efficient and reliable numerical techniques for the electromagnetic analysis and many numerical tools have been applied to the analysis of shielding effectiveness, such as finite Difference Time Domain (FDTD) (Jiao *et al*., 2006; Nuebel *et al*., 2000), finite Element Method (FEM) (Benhassine *et al*., 2002; Carpes *et al*., 2002), Method of Moments (MoM) (Wallyn *et al*., 2002; Wu *et al*., 2011), Transmission Line Matrix (TLM) (Podlozny *et al*., 2002; Attari and Barkeshli, 2002) and hybrid method (Wu *et al*., 2010) are utilised with good accuracy over a broad frequency band at the cost of large amount of computer memory and CPU time.

Deshpande introduced a moment method technique (modal MoM) using entire domain basis functions to represent apertures fields and therefore the magnetic currents on the apertures, which can evaluates the SE of a zero thickness enclosure exposed to a normally incident plane wave accurately at the center inside enclosure (Deshpande, 2000).This method has been further modified for obliquely polarimetric incident plane wave (ALI *et al*., 2005; Jayasree, 2010) and for finite wall thickness (Dehkhoda *et al*., 2009). As modal MoM is very fast and is an analytical solution in series form. It can yield arbitrary accuracy for increasing number of cavity modes (expanded in cavity Green's function) and increasing number of aperture modes in the rectangular aperture. These modes areexpanded in bases that form a complete set for this infinite Q-structure. It is useful for statistical investigation. Nowadays the EM shielding effectiveness has becoming a hot research point in the electromagnetic compatibility area (Bahadorzadeh and Moghaddasi, 2008; Robertson *et al*., 2008; Faghihi and Heydari, 2009; Koledintseva *et al*., 2009; Wang and Koh, 2004; Hussein, 2007; Morari *et al*., 2011; Kim *et al*., 2008; Bahadorzadeh and Moghaddasi, 2008; Fang *et al*., 2008).

In most of the aforementioned methods, the shielding effectiveness is calculated at the center of the enclosure. There are few studies that calculatedSE at other points inside enclosure and few SE studies in view

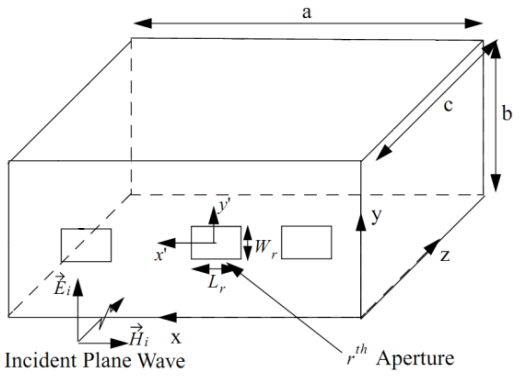


Fig. 1: Geometry of rectangular enclosure with rectangular apertures exposed to a normal incident plane wave

of apertures shape. In this paper, the modal MoM solution is formulated and by employing the surface equivalence principle and boundary conditions at each end of the aperture. Electric field SE is calculated at three different points inside enclosure with different shapes apertures, such as different rectangular apertures, square apertures. A very good agreement among the results of the proposed technique, results available in the literature and experimental results is observed. It is also shown that different calculation points severely affects the electric field SE, lower electric field SE near the aperture than at location inside the enclosure farther away from the aperture below the resonance frequency. Additionally, square apertures has higher SE than other shape apertures, even though they have the same area.

**Electromagnetic problem and the formulation of modal MOM:** The shielding effectiveness of an enclosure is defined as:

$$\text{SE(dB)}=-20\log\left(\frac{|\boldsymbol{E}_{\text{int}}|}{|\boldsymbol{E}_{\text{ext}}|}\right) \quad (1)$$

where, $\boldsymbol{E}_{\text{int}}$ is the electric fieldat a given point inside the enclosure, $\boldsymbol{E}_{\text{ext}}$ is the electric fieldat the same point in the absence of the enclosure. Therefore, the problem of estimation of shielding effectiveness is essentially the problem of calculating the cavity fields excited by a plane wave incident from free space upon the shielding enclosure.

Figure 1 shows a rectangular enclosure with rectangular apertures exposed to a normal incident plane wave. The dimensions of the cavity are $a \times b \times c$. There are r number of apertures and the dimensions of the rth aperture are $L_r \times W_r$. The orientation of the reference axes is also shown with the origin at the lower right corner of the front wall.

**Apertures fields and equivalent magnetic currents:** In the Modal MoM formulation, we assume that the apertures are relatively small compared to the walls in which they are located and are placed far enough away from the edges of the enclosure. In addition, the edge diffracted fields are neglected. These assumptions enable us to use image theory and equivalence principles, using the surface equivalence principle, the apertures both internal (Region I) and external (Region II) to the enclosure can be replaced by equivalent magnetic currents of:

$$M=n\times E_{apt} \tag{2}$$

where, $\boldsymbol{E}_{\text{apt}}$ is the tangential electric field induced on the apertures and n is the aperture normal vector.

$$\boldsymbol{E}_{apt}(\text{z}=0)=\sum_{r=1}^{R}\begin{bmatrix}\hat{y}\sum_p\sum_q U_{rpq}\sin\left(\frac{p\pi}{L_r}\left(\frac{L_r}{2}+x-x_{cr}\right)\right)\\ \times\cos\left(\frac{q\pi}{W_r}\left(\frac{W_r}{2}+y-y_{cr}\right)\right)\\ +\hat{x}\sum_p\sum_q V_{rpq}\cos\left(\frac{p\pi}{L_r}\left(\frac{L_r}{2}+x-x_{cr}\right)\right)\\ \times\sin\left(\frac{q\pi}{W_r}\left(\frac{W_r}{2}+y-y_{cr}\right)\right)\end{bmatrix} \tag{3}$$

where, $U_{rpq}$ and $V_{rpq}$ are the unknown amplitudes of the $pq$th mode of magnetic current on the outer of the $r$th aperture, $U_{rpq}\neq 0$ and $V_{rpq}\neq 0$ for $x_{cr}-\frac{L_r}{2}\leq x\leq x_{cr}+\frac{L_r}{2}$, $y_{cr}-\frac{W_r}{2}\leq y\leq y_{cr}+\frac{W_r}{2}$ and $U_{rpq}=V_{rpq}=0$ otherwise. $L_r$ and $W_r$ are the length and width of $r$th aperture, $x_{cr}$ and $y_{cr}$ are center coordinates of the $r$th aperture. $\hat{x},\hat{y}$ are the unit vectors in x, y directions. The unknown amplitudes $U_{rpq}$, $V_{rpq}$ are determined by setting up coupled integral equations.

Using the equivalence principle, the equivalent magnetic currents are:

$$\begin{aligned}\boldsymbol{M_{apt}}&=\boldsymbol{n_1}\times\boldsymbol{E}_{apt}\\ &=-\hat{z}\times\boldsymbol{E}_{apt}(\text{z}=0)\\ &=\sum_{r=1}^{R}\left[\hat{x}\sum_p\sum_q U_{rpq}\Psi_r-\hat{y}\sum_p\sum_q V_{rpq}\Phi_r\right]\\ &=\sum_{r=1}^{R}\boldsymbol{M}_{r1}\end{aligned} \tag{4}$$

where,

$$\Psi_r=\sin\left(\frac{p\pi}{L_r}\left(\frac{L_r}{2}+x-x_{cr}\right)\right)\times\cos\left(\frac{q\pi}{W_r}\left(\frac{W_r}{2}+y-y_{cr}\right)\right) \tag{5}$$

$$\Phi_r=\cos\left(\frac{p\pi}{L_r}\left(\frac{L_r}{2}+x-x_{cr}\right)\right)\times\sin\left(\frac{q\pi}{W_r}\left(\frac{W_r}{2}+y-y_{cr}\right)\right) \tag{6}$$

**Electromagnetic field outside enclosure:** Consider the aperture on the z=0 plane, the scattered EM field outside due to the rth aperture can be determined by solving electric vector potential:

$$\boldsymbol{E}=-\frac{1}{\varepsilon_0}\nabla\times\boldsymbol{F} \tag{7}$$

$$\boldsymbol{H}=-\frac{j\omega}{k_0^2}\left(k_0^2\boldsymbol{F}+\nabla\nabla\cdot\boldsymbol{F}\right) \tag{8}$$

Where the electric vector potential $\boldsymbol{F}$ is given by:

$$\boldsymbol{F}=\frac{\varepsilon_0}{4\pi}\iint_{apt}2\boldsymbol{M}_r\frac{e^{-jk_0|\boldsymbol{r}-\boldsymbol{r}'|}}{\boldsymbol{r}-\boldsymbol{r}'}ds \tag{9}$$

Superposition of the scattered electromagnetic field due to all apertures on the z = 0 plane gives the total scattered field as (Deshpande, 2000):

$$\begin{aligned}H_x^{\text{I}}=&\sum_{r=1}^{R}\sum_p\sum_q\frac{\omega\varepsilon_0}{4\pi^2k_0^2}\Big(U_{rpq}\int_{-\infty}^{\infty}\int_{-\infty}^{\infty}e^{-jk_z|z-z'|}\psi_{rpqy}\\ &\times\frac{k_0^2-k_x^2}{k_z}e^{jk_xx+jk_yy}dk_xdk_y-V_{rpq}\int_{-\infty}^{\infty}\int_{-\infty}^{\infty}e^{-jk_z|z-z'|}\\ &\times\phi_{rpqy}\frac{-k_xk_y}{k_z}e^{jk_xx+jk_yy}dk_xdk_y\Big)\end{aligned} \tag{10}$$

$$\begin{aligned}H_y^{\text{I}}=&\sum_{r=1}^{R}\sum_p\sum_q\frac{-\omega\varepsilon_0}{4\pi^2k_0^2}\Big(V_{rpq}\int_{-\infty}^{\infty}\int_{-\infty}^{\infty}e^{-jk_z|z-z'|}\phi_{rpqy}\\ &\times\frac{k_0^2-k_y^2}{k_z}e^{jk_xx+jk_yy}dk_xdk_y-U_{rpq}\int_{-\infty}^{\infty}\int_{-\infty}^{\infty}e^{-jk_z|z-z'|}\\ &\psi_{rpqy}\frac{-k_xk_y}{k_z}e^{jk_xx+jk_yy}dk_xdk_y\Big)\end{aligned} \tag{11}$$

$$\begin{aligned}H_z^{\text{I}}=&\\ &\sum_{r=1}^{R}\sum_p\sum_q\frac{-\omega\varepsilon_0}{4\pi^2k_0^2}\Big(\int_{-\infty}^{\infty}\int_{-\infty}^{\infty}e^{-jk_z|z-z'|}\left(U_{rpq}\psi_{rpqy}k_x-\right.\\ &\left.V_{rpq}\,\phi_{rpqy}k_y\right)e^{jk_xx+jk_yy}dk_xdy\end{aligned} \tag{12}$$

In expressions (10)-(12) $\phi_{\text{epgy}}$ ourier transform of $\Phi_{rpqy}$ and $\psi_{rpqy}$ is the Fourier transform of $\Psi_{rpqx}$.

**Eletromagnetic field inside enclosure** The equivalent magnetic currents, present on the apertures of the enclosure, radiate electromagnetic fields inside the enclosure. The total electromagnetic field at any point inside enclosure is obtained by a superposition of fields due to each equivalent magnetic current source. Considering the x- component of the magnetic current and using dyadic Green's function, The total magnetic field inside the enclosure is then obtained from (Deshpande, 2000) as:

$$H_x^{\mathrm{II}x0} = \frac{-j\omega}{k_0^2}\sum_{r=1}^{R}\sum_{p,q} U_{rpq}\sum_{m,n}^{\infty}\frac{-\varepsilon_0}{k_I}\frac{\varepsilon_{0m}\varepsilon_{0\mathrm{n}}}{ab\sin(k_I c)} \times\left(k_0^2-\left(\frac{\mathrm{m}\pi}{\mathrm{a}}\right)^2\right)\sin\left(\frac{m\pi x}{a}\right) \times\cos(\frac{n\pi y}{b})\cos(k_I(z-c))I_{rpq\mathrm{mn}x} \quad (13)$$

$$H_y^{\mathrm{II}x0} = \frac{-j\omega}{k_0^2}\sum_{r=1}^{R}\sum_{p,q} U_{rpq}\sum_{m,n}^{\infty}\frac{-\varepsilon_0}{k_I}\frac{\varepsilon_{0m}\varepsilon_{0\mathrm{n}}}{ab\sin(k_I c)} \times\frac{m\pi}{a}(-\frac{n\pi}{b})\cos\left(\frac{m\pi x}{a}\right) \times\sin\left(\frac{n\pi y}{b}\right)\cos\big(k_I(z-c)\big)I_{rpq\mathrm{mn}x} \quad (14)$$

$$H_z^{\mathrm{II}x0} = \frac{-j\omega}{k_0^2}\sum_{r=1}^{R}\sum_{p,q} U_{rpq}\sum_{m,n}^{\infty}\frac{-\varepsilon_0}{k_I}\frac{\varepsilon_{0m}\varepsilon_{0\mathrm{n}}}{ab\sin(k_I c)} \times\frac{m\pi}{a}(-k_I)\cos\left(\frac{m\pi x}{a}\right) \times\cos\left(\frac{n\pi y}{b}\right)\sin\big(k_I(z-c)\big)I_{rpq\mathrm{mn}x} \quad (15)$$

In (13)-(15),

$$I_{rpq\mathrm{mn}x} = \iint_q \Psi_{rpqx}(x',y')\sin\left(\frac{\mathrm{m}\pi x'}{\mathrm{a}}\right)\cos(\frac{n\pi y'}{b})dx'dy'$$

Likewise, considering the y-component of the magnetic current and using the proper boundary conditions, The total magnetic field inside the enclosure is then obtained from (Deshpande, 2000) as:

$$H_x^{\mathrm{II}y0} = \frac{-j\omega}{k_0^2}\sum_{r=1}^{R}\sum_{p,q} -V_{rpq}\sum_{m,n}^{\infty}\frac{-\varepsilon_0}{k_I}\frac{\varepsilon_{0m}\varepsilon_{0\mathrm{n}}}{ab\sin(k_I c)} \times(-\frac{m\pi}{a})\frac{n\pi}{b}\sin\left(\frac{m\pi x}{a}\right)\cos(\frac{n\pi y}{b}) \times\cos(k_{\mathrm{I}_r}(z-c))I_{rpq\mathrm{mn}y} \quad (16)$$

$$H_y^{\mathrm{II}y0} = \frac{-j\omega}{k_0^2}\sum_{r=1}^{R}\sum_{p,q} -V_{rpq}\sum_{m,n}^{\infty}\frac{-\varepsilon_0}{k_I}\frac{\varepsilon_{0m}\varepsilon_{0\mathrm{n}}}{ab\sin(k_I c)} \times\left(k_0^2-\left(\frac{n\pi}{b}\right)^2\right)\cos\left(\frac{m\pi x}{a}\right) \times\sin\left(\frac{n\pi y}{b}\right)\cos\big(k_I(z-c)\big)I_{rpq\mathrm{mn}y} \quad (17)$$

$$H_z^{\mathrm{II}y0} = \frac{-j\omega}{k_0^2}\sum_{r=1}^{R}\sum_{p,q} -V_{rpq}\sum_{m,n}^{\infty}\frac{-\varepsilon_0}{k_I}\frac{\varepsilon_{0m}\varepsilon_{0\mathrm{n}}}{ab\sin(k_I c)} \times\frac{n\pi}{b}(-k_I)\cos\left(\frac{m\pi x}{a}\right) \times\cos(\frac{n\pi y}{b})\sin(k_I(z-c))I_{rpq\mathrm{mn}y} \quad (18)$$

In (16)-(18),

$$I_{rpq\mathrm{mn}y} = \iint_q \Phi_{rpqy}(x',y')\cos\left(\frac{\mathrm{m}\pi x'}{\mathrm{a}}\right)\sin(\frac{n\pi y'}{b})dx'dy'$$

For a unique solution the electromagnetic fields in various regions satisfy continuity conditions over their common surfaces. The tangential electric fields over the apertures are continuous. The tangential magnetic over the apertures must also be continuous, thus yielding coupled integral equations with the magnetic currents as known variables. The coupled integral equation in conjunction with the method of moments can be solved for the amplitudes of magnetic currents.

**Derivation of integral equation:** The total tangential fields inside the cavity from apertures are written as:

$$\boldsymbol{H}_x^{II}=\boldsymbol{H}_x^{IIx0}+\boldsymbol{H}_x^{IIy0} \quad (19)$$

$$\boldsymbol{H}_y^{II}=\boldsymbol{H}_y^{IIx0}+\boldsymbol{H}_y^{IIy0} \quad (20)$$

Applying the continuity of tangential magnetic field on the z = 0 plane yields:

$$\boldsymbol{H}_x^I|_{z=0}+\boldsymbol{H}_{xi}|_{z=0}=\boldsymbol{H}_x^{II}|_{z=0} \quad (21)$$

$$\boldsymbol{H}_y^I|_{z=0}+\boldsymbol{H}_{yi}|_{z=0}=\boldsymbol{H}_y^{II}|_{z=0} \quad (22)$$

Now selecting $\Psi_{r'p'q'x}$ as a testing function and use of Galerkin's method reduces the (21) to:

$$I_{r'p'q'xi}=\sum_{r=1}^{R}\sum_{p,q}(U_{rpq}Y^{x1x1}_{rpqr'p'q'}+V_{rpq}Y^{x1y1}_{rpqr'p'q'}) \quad (23)$$

where,

$$Y^{x1x1}_{rpqr'p'q'}=\frac{-j\omega}{k_0^2}\sum_{m,n=0}^{\infty}\frac{-\varepsilon_0}{k_I}\frac{\varepsilon_{0m}\varepsilon_{0n}}{ab\sin(k_Ic)}$$

$$\left(k_0^2-\left(\frac{m\pi}{a}\right)^2\right)\cos(k_Ic)\,I_{rpqmnx}I_{r'p'q'mnx}+\frac{\omega\varepsilon_0}{4\pi^2k_0^2}\int_{-\infty}^{+\infty}\int_{-\infty}^{+\infty}\Psi_{rpqx}\Psi^*_{r'p'q'x}\frac{k_0^2-k_x^2}{k_z}dk_xdk_y \quad (24)$$

$$Y^{x1y1}_{rpqr'p'q'}=\frac{j\omega}{k_0^2}\sum_{m,n=0}^{\infty}\frac{-\varepsilon_0}{k_I}\frac{\varepsilon_{0m}\varepsilon_{0n}}{ab\sin(k_Ic)}\left(\frac{-m\pi}{a}\right)\left(\frac{n\pi}{b}\right)\times\cos(k_Ic)\,I_{rpqmny}I_{r'p'q'mnx}+\frac{\omega\varepsilon_0}{4\pi^2k_0^2}\int_{-\infty}^{+\infty}\int_{-\infty}^{+\infty}\phi_{rpqy}\,\psi^*_{r'p'q'x}\frac{-k_xk_y}{k_z}dk_xdk_y \quad (25)$$

$$I_{r'p'q'xi}=\iint_{r'p'q'}\boldsymbol{H}_{xi}\Psi_{r'p'q'x}\,dxdy \quad (26)$$

Similarly, selecting $-\Phi_{r'p'q'y}$ as a testing function and use of Galerkin's method reduces the (22) to:

$$I_{r'p'q'yi}=\sum_{r=1}^{R}\sum_{p,q}(U_{rpq}Y^{y1x1}_{rpqr'p'q'}+V_{rpq}Y^{y1y1}_{rpqr'p'q'}) \quad (27)$$

where

$$Y^{y1x1}_{rpqr'p'q'}=\frac{j\omega}{k_0^2}\sum_{m,n=0}^{\infty}\frac{-\varepsilon_0}{k_I}\frac{\varepsilon_{0m}\varepsilon_{0n}}{ab\sin(k_Ic)}\left(\frac{m\pi}{a}\right)\left(-\frac{n\pi}{b}\right)\times\cos(k_Ic)I_{rpqmnx}I_{r'p'q'mny}+\frac{\omega\varepsilon_0}{4\pi^2k_0^2}\int_{-\infty}^{+\infty}\int_{-\infty}^{+\infty}\psi_{rpqx}\Phi^*_{r'p'q'y}\frac{-k_xk_y}{k_z}dk_xdk_y \quad (28)$$

$$Y^{y1y1}_{rpqr'p'q'}=-\frac{j\omega}{k_0^2}\sum_{m,n=0}^{\infty}\frac{-\varepsilon_0}{k_I}\frac{\varepsilon_{0m}\varepsilon_{0n}}{ab\sin(k_Ic)}\times\left(k_0^2-\left(\frac{n\pi}{b}\right)^2\right)\cos(k_Ic)I_{rpqmny}I_{r'p'q'mny}-\frac{\omega\varepsilon_0}{4\pi^2k_0^2}\int_{-\infty}^{+\infty}\int_{-\infty}^{+\infty}\phi_{rpqy}\,\Phi^*_{r'p'q'y}\frac{(k_0^2-k_x^2)}{k_z}dk_xdk_y \quad (29)$$

$$I_{r'p'q'yi}=\iint_{r'p'q'}\boldsymbol{H}_{yi}\Phi_{r'p'q'x}\,dxdy \quad (30)$$

Equation (23) and (27) can be written in a matrix form as:

$$\begin{bmatrix}Y^{x1x1}_{rpqr'p'q'} & Y^{x1y1}_{rpqr'p'q'}\\ Y^{y1x1}_{rpqr'p'q'} & Y^{y1y1}_{rpqr'p'q'}\end{bmatrix}\begin{bmatrix}U_{rpq}\\ V_{rpq}\end{bmatrix}=\begin{bmatrix}I_{r'p'q'xi}\\ 0\end{bmatrix} \quad (31)$$

The matrix Eq. (31) can be numerically solved for the unknown amplitudes of equivalent magnetic currents induced on the apertures due to given incident field. From the knowledge of these amplitudes electromagnetic field inside as well as outside the enclosure can be obtained.

**Validation of the present technique:** In this section, for the validation of the presented method, we consider a rectangular enclosure of size (30× 12 × 30 $cm$) with arectangular aperture of size (10 0.5 cm) located at

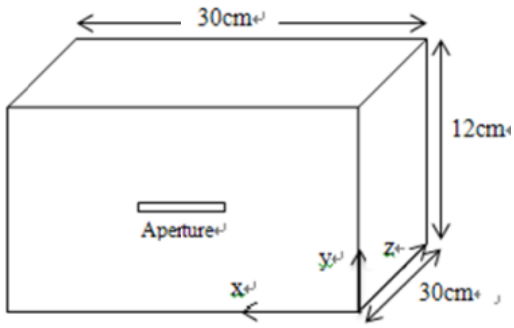


Fig. 2: Geometry of 30cm × 12cm × 30cm enclosure with a single aperture at (15cm, 6cm, 0)

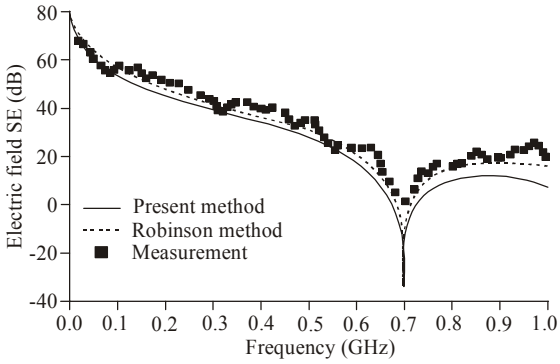


Fig. 3: Electric field SE calculated at the center of 30×12×30 cm enclosurewith a 10×0.5 cm aperture located at 15×6 cm in z = 0 plane illuminated by vertical polarized plane wave

the center of the front wall (15, 6cm, 0), as illustrated in Fig. 2. The enclosureis illuminated by a normal incident plane wave at 0 polarization.

Assuming only expansion mode on the aperture and considering only dominantmode inside the cavity. the shielding effectiveness is calculated at the center of the cavity. electric field shielding obtained using expression (31) is plotted in Fig. 3 along with the results from (Robinson *et al*., 1998). It is observed that the numerical data obtained using the present method agrees well with the earlier published results. Experimental data from (Robinson *et al*., 1998) is also reproduced in Fig. 3.

## RESULTS AND DISCUSSION

In this section, in order to study the electric field shielding effectiveness versus different calculation points in the enclosure, a 30 12 30 cm enclosurehaving two types of apertures with the same area is selected. The enclosure is illuminated by a normal incident plane wave at 0 polarization.

Figure 4 presents the plot of electric field shielding effectiveness versus three different points inside the enclosure with two types of apertures. We note that increasing the frequency decreases the shielding effectiveness and the resonance frequency of the cavity is about 0.7 GHz. Also note that the maximum and minimum of electric field SE below the resonance frequency occur at z = 250 mm and z = 50 mm respectively in Fig. 4a, the maximum difference of electric field SE is almost 20dB, which is in accordance with the usual assumption made in EMC literature that lower electric field SE near the aperture than at location inside the enclosure farther away from the aperture, but

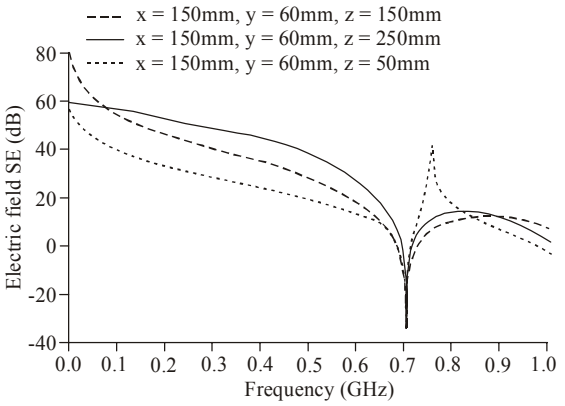


(a)

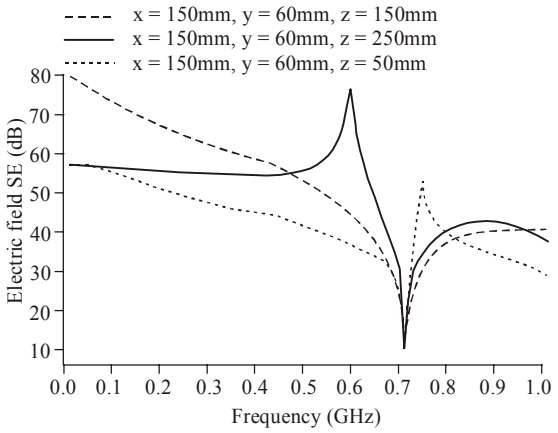


(b)

Fig. 4: Electric field shielding calculated at different points inside 30×12×30 cm enclosure with two types of apertures located at 15×6 cm in z = 0 plane illuminated by vertical polarized plane wave a: 10.0× 0.5 cm aperture; b: 2.23×2.23 cm aperture

when the frequency exceed the resonance frequency, this result is wrong.

The most interesting observation that can be made for electric field SE in Fig. 5b is that the electric field SE under 0.46 GHz at z = 50 mm is higher than the others, which is not similar with the usual assumption. We also note that electric field SE increase rapidly to more than 40dB at 0.75GHz on the z = 50cm point because of modal structure of the fields. A particular case is that the electric field SE of 2.23×2.23 cm aperture at z = 250mm has also a rapid increase at about 0.59GHz.

In this section, we discuss electric field SE results calculated at three different points versus different shapes apertures. We also consider a $30\text{cm} \times 12cm \times$

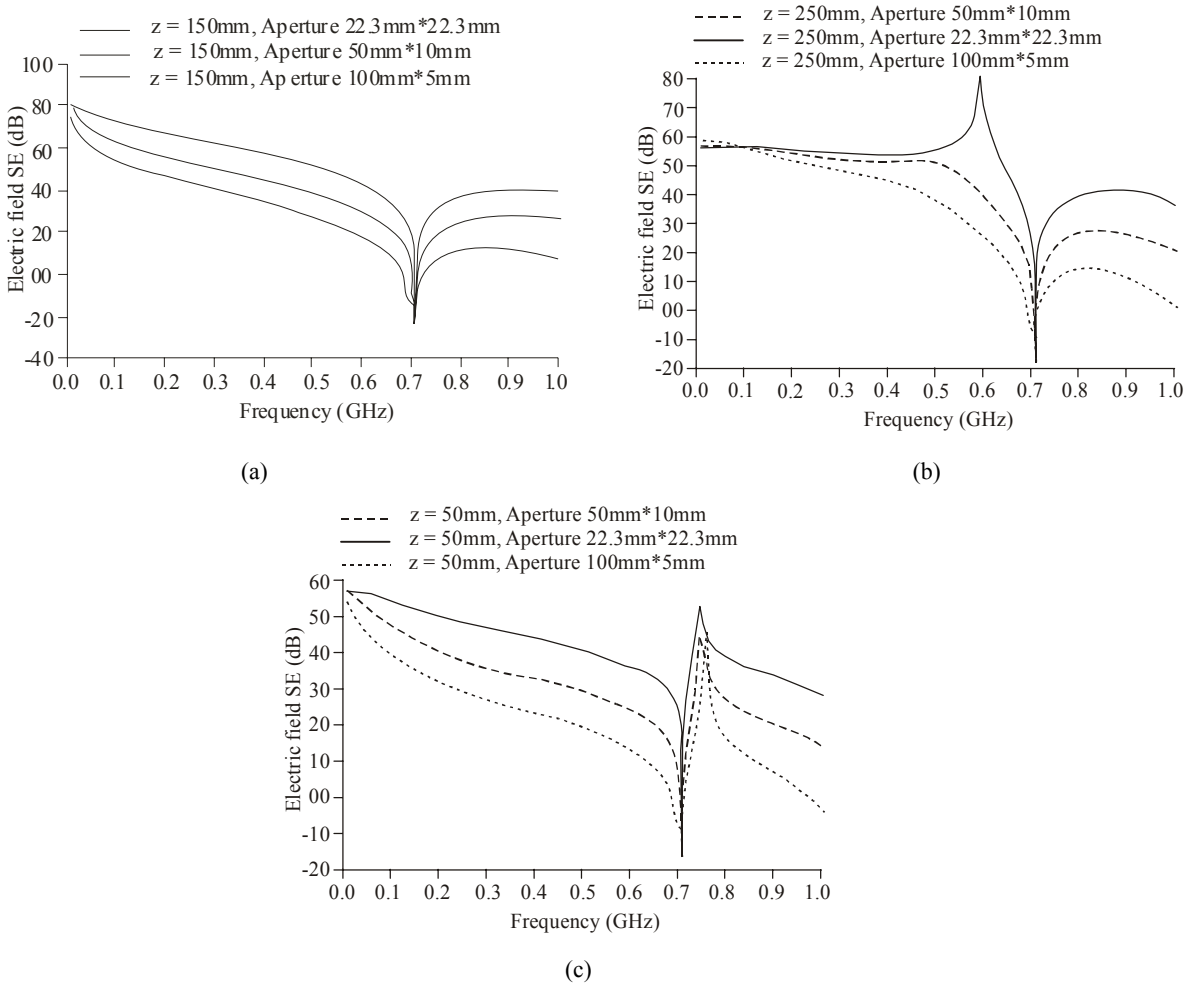


Fig. 5: Electric field SE calculated at different points inside 30×12×30 cm enclosure with a aperture of size (10×0.5 cm, 5.0×1.0 cm and 2.23×2.23 cm) located at 15×6 cm in z = 0 plane illuminated by vertical polarized plane wave a: Electric fieldSE calculated at z = 150 mm, x = 150 mm, y = 60 mm; b: Electric field SE calculated at z = 250 mm, x = 150 mm, y = 60 mm; c: Electric fieldSE calculated at z = 50 mm, x = 150 mm, y = 60 mm

30 cm enclosure with rectangular aperture of size (10 0.5 cm, 5.0 1.0cm and 2.23 2.23 cm) located at the center ofthe front wall (15 cm, 6 cm, 0) respectively. The enclosureis illuminated by a normal incident plane wave at 0 polarization.

Fig. 5a, b and c presents three plots of electric field SE versus three different shapes aperture with same area respectively. We observe a similar changed trend in Fig. 5a, b and c that all the resonance frequency is about 0.7 GHz, electric field SE increase in turn from 10.0cm×0.5cm aperture to 2.23×2.23cm aperture and electric field SE have a rapid increase up to about 50dB at 0.75GHz at z = 50 mm because of modal structure of the fields. Figure 5 confirms the electric field SE dependence upon distance from the apertures. We also note that the apertures with different shape but same area have different effect on electric field SE. For one aperture case, from discussed above, we can conclude that square aperture have higher electric field SE than rectangular aperture when their area is same.

Figure 6 presents six plots of electric field SE versus two types of apertures with the same area at different calculation points in the cavity. We observe that the electric field SE have a similar changed trend in two types of apertures at all frequency and the electric field SE of two apertures is higher than that of one aperture while they have the same area. The results indicate that two apertures is a better select to improve the shielding ability of an enclosure than one aperture while they have the same area.

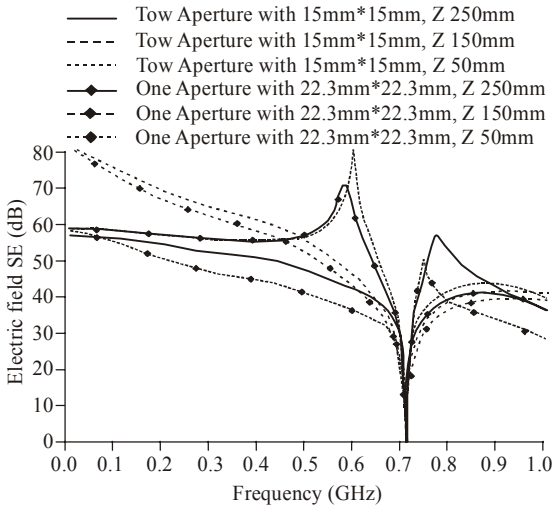


Fig. 6: Electric field SE calculated at different points inside 30×12×30 cm enclosure havinga 2.23×2.23 cm aperturelocated at 15×6 cm in z = 0 planeand two 1.5×1.5 cm apertures located at 20×6 cm and 10×6 cm in z = 0 plane respectively illuminated by vertical polarized plane wave

## CONCLUSION

In this study, an investigation on the effects of different calculation point inside the enclosure and different shape apertures on the electric field shielding effectiveness of metallic rectangular enclosures illuminated by vertical polarized plane waves has been carried out. For this purpose, the modal MoM solution is formulated and by employing the surface equivalence principle and boundary conditions at each end of the aperture, the problem is solved. Numerical results on electric field shielding effectiveness of a rectangular enclosure are good agree with data available in the literature. The results of the present analysis show that electric field SE of 10.0× 0.5 cm aperture is in accordance with the usual assumption made in EMC literature that lower electric field SE near the aperture than at location inside the enclosure farther away from the aperture. But for the electric field SE of 2.2 2.23 cm aperture, the assumption is not true. Additionally, square apertures has higher SE than other shape apertures, even though they have the same area. For the same area of aperture, the electric field SE of two apertures is higher than that of one aperture. These useful results gained in this study have the important practical significance to improving the electric field shielding effectiveness of shielding cavity.

## ACKNOWLEDGMENT

This study was supported by National Science funds of Civil Aviation Flight University of China (serial number: J2007-23) and Open Funds of CAAC academy of flight technology and safety.

## REFERENCES

Ali, K.Z., C.F. Bunting and M.D. Deshpande, 2005. Shielding effectiveness of metallic enclosures at oblique and arbitrary polarizations. IEEE Trans. Electromagn. Compat., 47(1): 112-122.

Arvas, E. and R.F. Harrington, 1983. Computation of the magnetic polarizability of conducting disks and the electric polarizability of apertures. IEEE Trans. Antennas Propagat., AP-31(5): 719-725.

Attari, R. and K. Barkeshli, 2002. Application of the transmission line matrix method to the calculation of the shielding effectiveness for metallic enclosures. Proceeding of IEEE Antennas Propagation Social International Symp., 3: 302-305.

Bahadorzadeh, M. and M.N. Moghaddasi, 2008. Improving of shielding effectiveness of a rectangular metallic enclosure with aperture by using extra wall. Prog. Electromagn. Res. Lett., 1: 45-50.

Bethe, H.A., 1944. Theory of diffraction by small holes. Phys. Rev., 66: 163-182.

Belokour, D.W.P., J. LoVetri and S. Kashyap, 2001. A higher order mode transmission linemodel of the shielding effectiveness of enclosures with apertures. Proceeding of IEEE International Symp. Electromagnetic Compatibility, 2(13-17): 702-707.

Benhassine, S., L. Pichon and W. Tabbara, 2002. An efficient finite-element time-domain method for the analysis of the coupling between wave and shielded enclosure. IEEE Trans. Magn., 38(2): 709-712.

Carpes Jr, W.P., L. Pinchon and A. Razek, 2002. Analysis of the coupling of an incident wave with a wire inside a cavity using an FEM in frequency and time domains. IEEE Trans. Electromagn. Compat., 44(3): 470-475.

Deshpande, M.D., 2000. Electromagnetic field Penetration Studies (NASA/CR-2000-210 297). [Online]. Retrieved from: http://techre-orts.larc.nasa.gov/ ltrs/PDF/2000 /cr/ NASA-2000-cr210 297.pdf.

Dehkhoda, P., A. Tavakoli and R. Moini, 2009. Shielding effectiveness of a rectangular enclosure with finite wall thickness and rectangular apertures by the generalized modal method of moments. IEET Sci. Meas. Technol., 3(2): 123-136.

Fang, C.H., S.Q. Zheng, H. Tan, D.G. Xie and Q. Zhang, 2008. Shielding effectiveness measurements on enclosures with various apertures by both mode-tuned reverberation chamber and gtem cell methodologies. Prog. Electromagn. Res. B, 2: 103-114.

Faghihi, F. and H. Heydari, 2009. Reduction of leakage magnetic field in electromagnetic systems based on active shielding concept verified by eigenvalue analysis. Prog. Electromagn. Res., PIER 96: 217-236.

Hussein, K.F.A., 2007. Effect of internal resonance on the radar cross section and shield effectiveness of open spherical enclosures. Prog. Electromagn. Res., PIER 70: 225-246.

Jiao, C., X. Cui, L. Li and H. Li, 2006. Subcell FDTD analysis of shielding effectiveness of a thin-walled enclosure with an aperture. IEEE Trans. Magn., 42(4): 1075-1078.

Jayasree, P.V.Y., 2010. Analysis of shielding effectiveness of single, double and laminated shields for oblique incidence of EM waves. Prog. Electromagn. Res. B, 22: 187-202.

Kim, Y.J., U. Choi and Y.S. Kim, 2008. Screen filter design consideration for Plasma Display Panels (PDP) to Achieve a high brightness with a minimal loss of EMI shielding effectiveness. J. Electromagn. Waves Appl., 22(5-6): 775-786.

Koledintseva, M.Y., J. Drewniakand and R. DuBroff, 2009. Modeling of shielding composite materials and structures for microwave frequencies. Prog. Electromagn. Res. B, 15: 197-215.

McDonald, N.A., 1985. Polynomial approximations for the electric polararizabilites of some small apertures. IEEE Trans. Microwave Theory Tech., MTT-33(11): 1146-1149.

Mendez, H.A., 1978. Shielding theory of enclosures with apertures. IEEE Trans. Electromagn.Compat., EMC-20: 296-305.

Mendez, H.A., 1974. On the theory of low-frequency excitation of cavity resonances. IEEE Trans. Microwave Theory Tech., MTT-18: 444-448.

Morari, C., I. Balan, J. Pintea, E. Chitanu and I. Iordache, 2011. Electrical conductivity and electromagnetic shielding effectiveness of silicone rubber filled with ferrite and graphite powders. Prog. Electromagn. Res. M, 21: 93-104.

Nuebel, M., J. Li, J.L. Drewniak, T.H. Hubing, R.E. DuBroff and T.P. Van Doren, 2000. EMI from cavity modes of shielding enclosures-FDTD modeling and measurements. IEEE Trans. Electromagn. Compat., 42(1): 29-38.

Podlozny, V., C. Christopoulos and J. Paul, 2002. Efficient description of fine features using digital filters in time domain computational electromagnetic. IEET Sci. Meas. Technol., 149(5): 254-257.

Robinson, M.P., J.D. Turner, D.W.P. Thomas, J.F. Dawson, M.D. Ganley, A.C. Marvin, S.J. Porter, T.M. Benson and C. Christopolous, 1996. Shielding effectiveness of a rectangular enclosure with a rectangular aperture. Electron. Lett., 32(17): 1559-1560.

Robinson, M.P., T.M. Benson, C. Christopoulos, J.F. Dawson, M.D. Ganley, A.C. Marvin, S.J. Porter and D.W.P. Thomas, 1998. Analytical formulation for the shielding effectiveness of enclosures with apertures. IEEE Trans. Electromagn. Compat., 40(3): 240-248.

Robertson, J., E.A. Parker, B. Sanz-Izquierdo and J.C. Batchelor, 2008. Electromagnetic coupling through arbitrary apertures in parallel conducting planes. Prog. Electromagn. Res. B, 8: 29-42.

Thomas, D.W.P., A. Denton, T. Konefal, T.M. Benson, C. Christopoulos, J.F. Dawson, A.C. Marvin and J. Porter, 1999. Characterization of the shielding effectiveness of loaded equipment enclosures. In Proceeding of International Conference Expo. EMC, pp: 89-94.

Wang, Y.J. and W.J. Koh , 2004. Coupling cross section and shielding effectiveness measurements on a coaxial cable by both mode-tuned reverberation chamber and gtem cell methodologies. Prog. Electromagn. Res., PIER 47: 61-73.

Wallyn, W., D. De Zutter and H. Rogier, 2002. Prediction of the shielding and resonant behavior of multisection enclosures based on magnetic current modeling. IEEE Trans. Electromagn. Compat., 44(1): 130-138.

Wu, G., X.G. Zhang and B. Liu, 2010. A hybrid method for predicting the shielding effectiveness of rectangular metallic enclosures with thickness apertures. J. Electromagn. Waves Appl., 24(8-9): 1157-1169.

Wu, G., X.G. Zhang, Z.Q. Song and B. Liu, 2011. Analysis on Shielding Performance of Metallic Rectangular Cascaded Enclosure with Apertures. Prog. Electromagn. Res. Lett., 20: 185-195.